6748 *Inorg. Chem.* **2010**, *49*, 6748–6754
DOI: 10.1021/ic100874r

Inorganic Chemistry
Article

Na_2SO_4 Monocrystal Nanowires—Aspect Ratio Control and Electron Beam Radiolysis

Ruiting Zheng,[†,‡] Jinwei Gao,[†,§] Tengfei Yang,[‡] Yucheng Lan,[∥] Guoan Cheng,[‡] Dezhi Wang,[∥] Zhifeng Ren,[∥] and Gang Chen*[,†]

[†]*Department of Mechanical Engineering, Massachusetts Institute of Technology, Cambridge, Massachusetts 02139* , [‡]*Key Laboratory of Radiation Beam Technology and Materials Modification of Ministry of Education, College of Nuclear Science and Technology, Beijing Normal University; Beijing, 100875, China,* [§]*School of Physics and Telecommunication Engineering, South China Normal University, Guangzhou, 510631, China, and* [∥]*Department of Physics, Boston College, Chestnut Hill, Massachusetts 02467*

Received May 3, 2010

This paper presents the synthesis of water-dissolvable Na_2SO_4 nanowires and nanorods by a simple chemical reaction between $CuSO_4$ and $NaBH_4$ in ethylene glycol. By adjusting the pH and the monomer concentration, the aspect ratio and size of the Na_2SO_4 nanowires could be tuned. Na_2SO_4 nanorods, nanowhiskers, nanowires, and submicrorods were obtained. Optimal chemical potential is believed to be the dominant driving force for the growth of Na_2SO_4 nanowires during the synthesis. We also demonstrated the Na_2SO_4 nanotubes obtained by the electron beam radiolysis of Na_2SO_4 nanowires. The mechanism of selective radiolysis is also investigated.

1. Introduction

Crystallization and physical properties of inorganic salt crystals have been well studied. Compared with bulk crystals, however, less research has been carried out on inorganic salt nanocrystals. Recently, NaCl, Na_2SO_4, and Na_2CO_3 inorganic salt nanocrystal arrays have been obtained by microengineering the shape of nanocrystals in a microchannal[1] or a microwell.[2] Water-dissolvable Na_2SO_4 nanowires[3] and $(NH_4)_2PtCl_6$ microcrystals[4] have been adopted as templates to synthesize hollow micro/nano structures. Such salt-based templates are advantageous compared to using other water-insoluble nanowires and nanoparticle as templates[5] that require selective etching or calcinating in the subsequent template removal, in terms of simplicity, environmental impacts, and costs. However, the growth mechanism and shape control of inorganic salt nanocrystals still await further investigation.

In this paper, we investigate the growth mechanism of Na_2SO_4 nanowires and report a simple technique to control the aspect ratio and diameter of Na_2SO_4 nanowires at room temperature. We also report Na_2SO_4 nanotubes obtained by the electron beam (EB) radiolysis of the Na_2SO_4 nanowires. Na_2SO_4 is an environmentally friendly and a water-dissolvable inorganic salt that can be easily removed by water. Hence, Na_2SO_4 nanorods, nanowhiskers, nanowires, submicrometer rods, and nanotubes reported in this paper can be ideal candidate templates for the synthesis of hollow structures for many other applications.

2. Experimental Section

2.1. Reagent. Copper sulfate pentahydrate ($CuSO_4 \cdot 5H_2O$, 99%), sodium borohydride ($NaBH_4$, 98%), hydrochloric acid (HCl, 10% V/V aqueous solution), sodium chloride (NaCl, 99.0%), sodium hydroxide (NaOH, 50% w/w aqueous solution), and ethanol (anhydrous, 94−96%) were purchased from Alfa Aesar and used without further purification. Polyvinylpyrrolidone (PVP) (K30, molecular weight of 40 000) and ethylene glycol (EG) (anhydrous, 99.8%) were purchased from Sigma-Aldrich. Deionized water was purchased from Mallinckrodt Baker.

2.2. Growth of Na_2SO_4 Nanowires. Na_2SO_4 nanowires were prepared by the reaction of $CuSO_4$ with $NaBH_4$ at room temperature. Typically, 0.25 g $CuSO_4 \cdot 5H_2O$ and 1 mmol PVP (in repeating unit,) are dissolved in 50 mL EG to form a homogeneous solution. Then 0.15 g $NaBH_4$ is added into the solution, under vigorous stirring. The color of the solution changed from bluish to brown in 2 min. After 30 min, there were no bubbles generated in the solution, indicating that the

*Corresponding author. Telephone: 1-617-253-0006. Fax: 1-617-258-5802. E-mail: gchen2@mit.edu.

(1) Suh, K. Y.; Khademhosseini, A.; Eng, G.; Langer, R. *Langmuir* **2004**, *20*, 6080–6084.
(2) Sato, Y.; Koide, Y. *Chem. Lett.* **2009**, *38*, 674–675.
(3) Pu, Y. C.; Hwu, J. R.; Su, W. C.; Shieh, D. B.; Tzeng, Y.; Yeh, C. S. *J. Am. Chem. Soc.* **2006**, *128*, 11606–11611.
(4) Lou, X. W.; Yuan, C.; Zhang, Q.; Archer, L. A. *Angew. Chem., Int. Ed.* **2006**, *45*, 3825–3829.
(5) (a) Tenne, R.; Rao, C. N. R. *Philos. Trans. R. Soc., A* **2004**, *362*, 2099–2125. (b) Bommel, K. J. C.; Friggeri, A.; Shinkai, S.; Bommel, K. J. C; Friggeri, A.; Shinkai, S. *Angew. Chem., Int. Ed.* **2003**, *42*, 980–999. (c) Lou, X. W.; Archer, L. A.; Yang, Z. *Adv. Mater.* **2008**, *20*, 3987–4019.

 Published on Web 06/15/2010

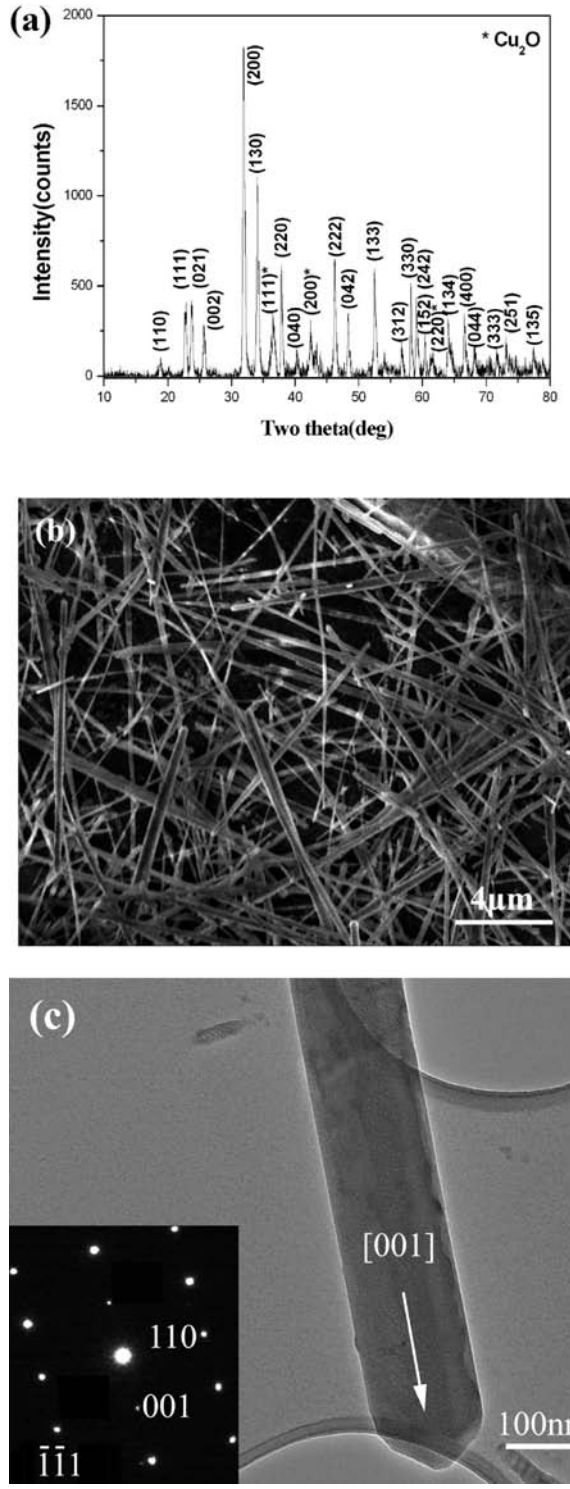

Figure 1. Microstructure characterization of as-prepared nanowires. (a) XRD pattern of the as-prepared nanowires. (b) SEM image of the Na_2SO_4 nanowires. (c) TEM image and SAED pattern of a nanorod grown along the [001] direction.

reaction was complete. The aspect ratio of Na_2SO_4 nanowires was tuned by the adjustment of reactant concentration and pH of the $CuSO_4$ solution in the range of 2−7 with HCl. The as-prepared products were centrifuged from the solution at 4000 rpm for 15 min by a Marathon21000 centrifuger (Fisher Scientific). The derived products were washed with ethanol three times to get the white reaction products and were preserved in ethanol as a suspension. Transmission electron microscopy (TEM) samples were prepared by dispersing a drop of the above suspension

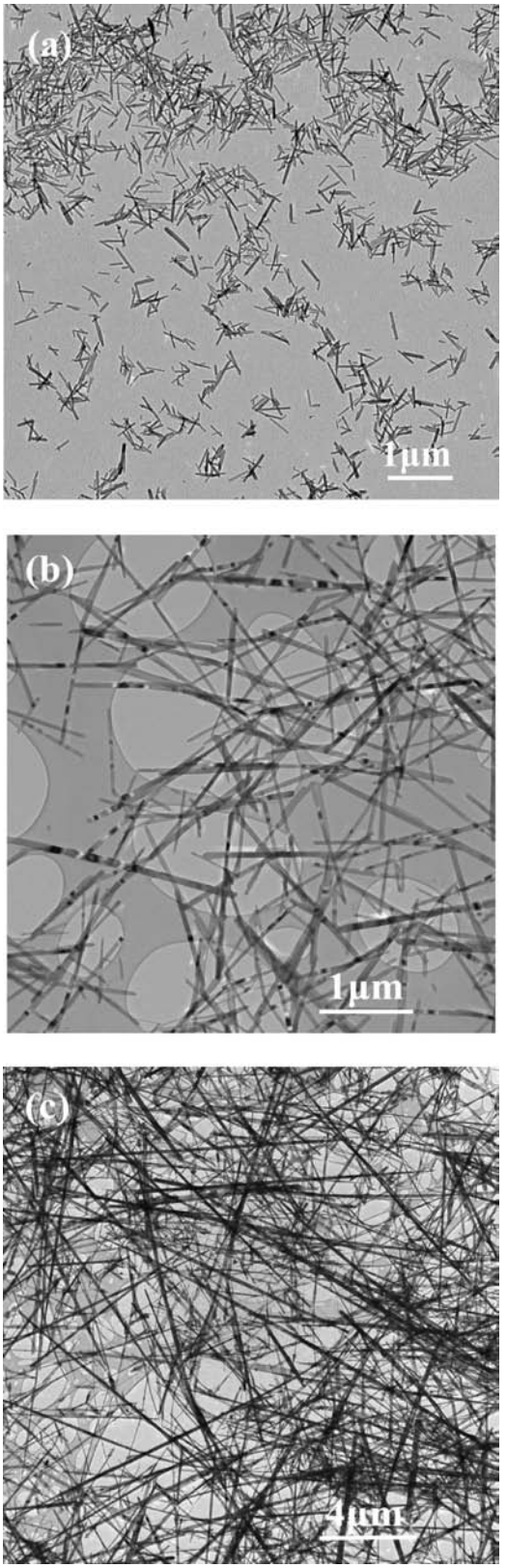

Figure 2. TEM images of Na_2SO_4 nanowhiskers with different aspect ratios. (a) Na_2SO_4 nanorods with an average aspect ratio of 12, (b) Na_2SO_4 nanowires with an average aspect ratio of 26, and (c) Na_2SO_4 nanowires with an average aspect ratio exceeding 100.

on carbon films supported by copper grids. The pH in solution is measured by an Exstik pH meter (Exstik pH100, EXTECH Instrument Corporation). All the synthesis conditions and the products are listed in the Supporting Information, Table S1.

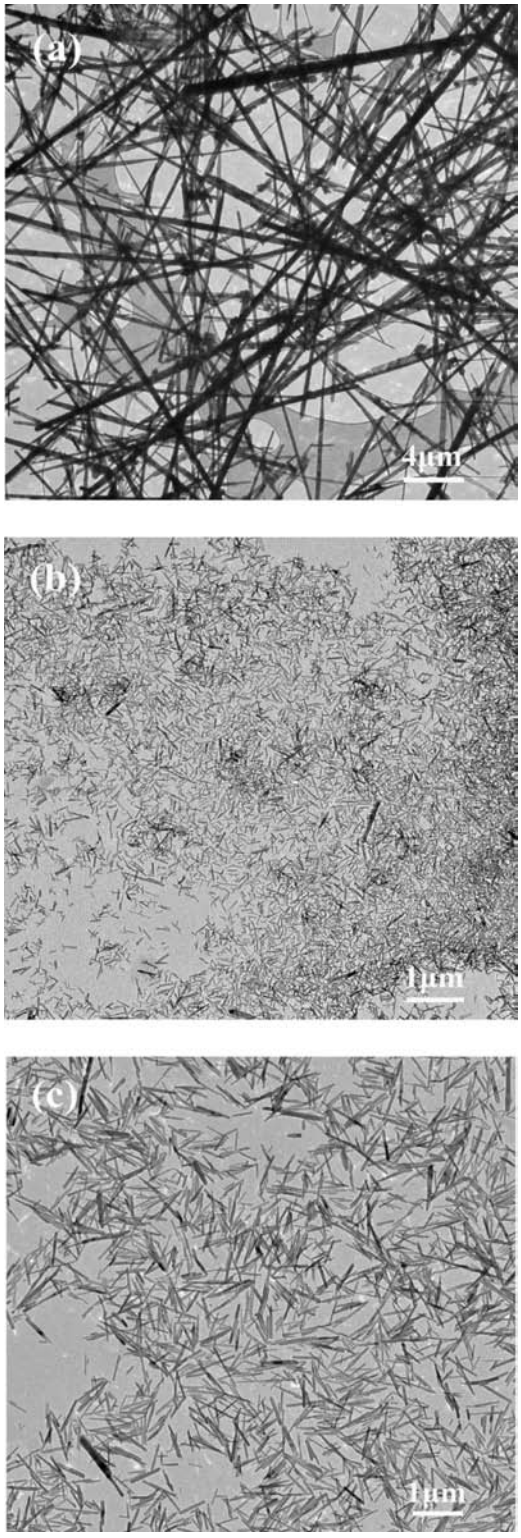

Figure 3. TEM images of Na_2SO_4 nanowires and nanorods prepared by different processes. (a) Na_2SO_4 nanowires obtained by the reaction of $CuSO_4$ and $NaBH_4$ with the addition of PVP and two drops of 0.1 M NaCl solution; (b) Na_2SO_4 nanorods obtained by the reaction of H_2SO_4 and NaOH in EG with the existence of PVP; and (c) Na_2SO_4 nanorods obtained by the reaction of $CuSO_4$ and $NaBH_4$ in EG without the help of PVP.

2.3. Microstructure Characterization and EB Radiolysis of Na_2SO_4 Nanowires. Crystal structures of the Na_2SO_4 nanowires were identified by a powder X-ray diffractometer (XRD) (Rigaku RU300, Japan), employing Cu Kα radiation ($\lambda = 1.5418$ Å) at 50 kV and 300 mA. The sizes and morphologies of the Na_2SO_4 nanowires were observed by a field emission scanning electron microscopy (SEM) (JEOL 6320, Japan) at 5 kV. Crystal structure and growth orientation of the Na_2SO_4 nanowires were characterized by TEM (JEOL JEM 200CX, Japan) at 200 kV and high-resolution transmission electron microscopy HRTEM (JEOL 2010 and JEOL 2011, Japan) at 200 kV. The EB radiolysis of Na_2SO_4 nanowires was carried out by both TEM and HRTEM.

3. Results and Discussions

Figure 1 illustrates the microstructures of typical Na_2SO_4 nanowires synthesized at pH = 3. Figure 1a is the XRD pattern of a reaction product in the 2θ range of 10−80°. The pattern could be distinctly indexed to an orthorhombic phase with lattice constants $a = 5.607$, $b = 8.955$, and $c = 6.967$ Å for Na_2SO_4 (Joint Committee on Powder Diffraction Standards (JCPDS) no. 83-1570). A little residual cubic phase Cu_2O with lattice constant $a = 4.26$ Å (JCPDS no. 71-4310) was also observed, which could be removed by a gradient centrifugation technique. Different from both prism and needle Na_2SO_4 crystals grown from aqueous solution at room temperature,[6] the precipitates obtained in our experiment were all Na_2SO_4 nanowires. SEM observation of the precipitates is illustrated in Figure 1b. The precipitates exhibit typical wire morphology with diameters of 100−300 nm and with aspect ratios exceeding 100. Selected area electron diffraction (SAED) patterns of Na_2SO_4 nanowires, as shown in Figure 1c, reveal the single crystalline nature of the nanowires. The preferred growth direction of these Na_2SO_4 nanowires was determined to be along the [001] direction, i.e., *c* axis of orthorhombic phase. The space group of our Na_2SO_4 nanowires is *Cmcm*, (001) has a zero XRD intensity because of systematic extinction, (002) has a nonzero structure factor, and can be detected.

The aspect ratio of Na_2SO_4 nanowires could be tuned by adjusting the reactant concentration and pH of the $CuSO_4$ solution. Figure 2a shows the TEM image of reaction products prepared by the reaction of 0.125 g $CuSO_4 \cdot 5H_2O$ and 0.075 g $NaBH_4$ in EG at pH = 7. Na_2SO_4 nanorods with a diameter of 20−50 nm and an aspect ratio of 9−15 were observed. Figure 2 b illustrates the TEM image of reaction products synthesized by the reaction of 0.25 g $CuSO_4 \cdot 5H_2O$ and 0.15 g $NaBH_4$ in EG at pH = 7. Na_2SO_4 nanowhiskers with diameters of 70−120 nm and aspect ratios of 19−33 were produced. If the reaction of 0.25 g $CuSO_4 \cdot 5H_2O$ and 0.15 g $NaBH_4$ was performed in EG at pH = 3, then Na_2SO_4 nanowires with diameters of 100−300 nm and average aspect ratios exceeding 100 could be obtained (Figure 2c).

We speculate that Na_2SO_4 tends to form nanowires due to an orientational crystallization mechanism.[7] With the help of H_2O molecules that existed in $CuSO_4 \cdot 5H_2O$ crystal, $CuSO_4$ could be dissolved in EG and form a uniform ionic solution. When the $NaBH_4$ is added in the solution, the bluish Cu^{2+} is reduced into yellowish Cu_2O nanoparticles, and H_2 is generated. At the same time, Na_2SO_4 nanorods will homogeneously nucleate from the solution, because the solvability of Na_2SO_4 in EG is extremely low at room temperature.[8]

(6) Amirthalingam, V.; Karkhanavala, M. D.; Rao, U. R. K. *Acta Crystallogr*. **1977**, *A33*, 522–532.
(7) (a) Peng, Z. A.; Peng, X. G. *J. Am. Chem. Soc*. **2001**, *123*, 1389–1395. (b) Peng, Z. A.; Peng, X. G. *J. Am. Chem. Soc*. **2002**, *124*, 3343–3353. (c) Wang, X.; Li, Y. *Angew. Chem., Int. Ed*. **2002**, *41*, 4790–4793.
(8) (a) Vener, R. E.; Thompson, A. R. *Ind. Eng. Chem*. **1949**, *41*, 2242–2247. (b) Vener, R. E.; Thompson, A. R. *Ind. Eng. Chem* **1950**, *42*, 171–174.

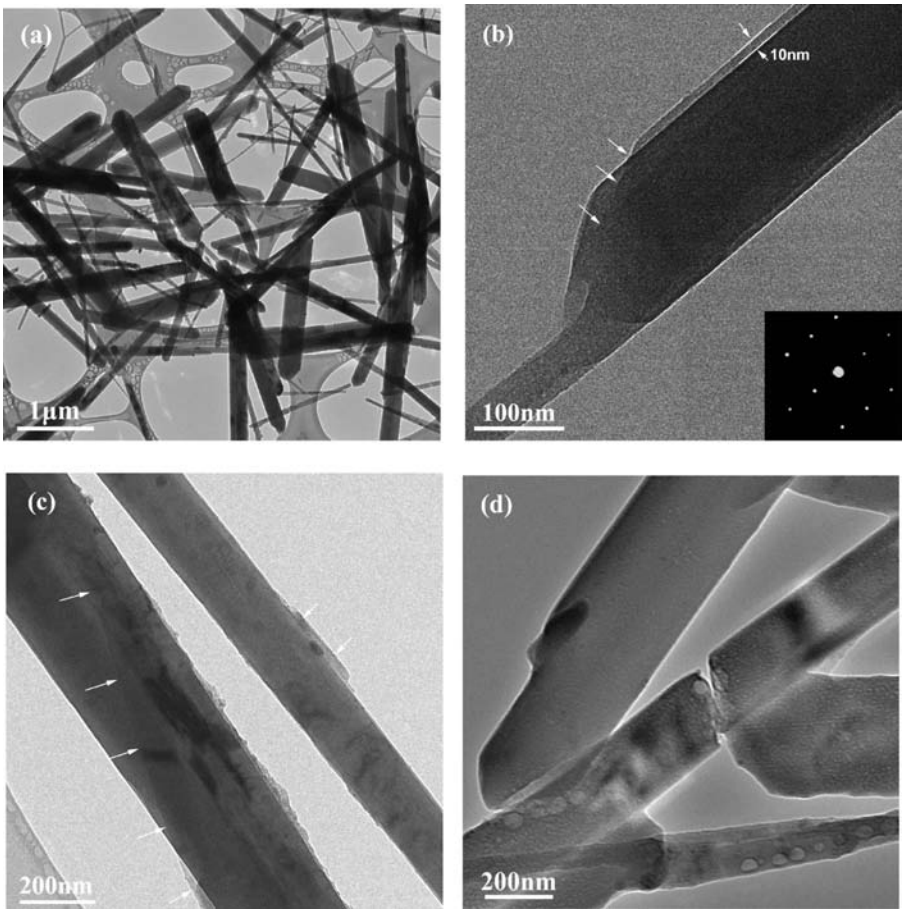

Figure 4. TEM images of Na_2SO_4 submicrorods. (a) Morphology of Na_2SO_4 submicrorods; (b) a typical end structure of a Na_2SO_4 submicrorod, the inset is the SAED pattern of this submicrorod, and the white arrows show the thickness of the outer layer is about 10 nm; (c) growth edges of the Na_2SO_4 outer layer indicated by arrows; and (d) the transmission image of a broken Na_2SO_4 submicrorod.

The reactions can be expressed as[9]

$$NaBH_4 + 2C_2H_6O_2 \rightarrow Na^+ + B(C_2H_4O_2)_2^- + 4H_2\uparrow$$

$$2Cu^{2+} + 2NaBH_4 + 5H_2O \rightarrow Cu_2O\downarrow + 2Na^+ + 2BO_2^- + 7H_2\uparrow + 4H^+$$

$$2Na^+ + SO_4^{2-} \rightarrow Na_2SO_4\downarrow$$

Like other orthorhombic one-dimensional nanostructures,[10] Na_2SO_4 tends to form nanorods when it precipitates from the solution, because of the highly anisotropic nature of the Na_2SO_4 orthorhombic structure. The first-precipitated Na_2SO_4 nanorods could serve as seeds. When subsequent Na_2SO_4 monomers precipitate from the solution, they tend to aggregate along the *c* axis of the seeds and grow up. At low Na_2SO_4 monomer concentrations, only nanorods can be obtained, as indicated in Figure 2a, since the diffusion of Na_2SO_4 monomers is not fast enough. With the increase of Na_2SO_4 monomer concentrations, Na_2SO_4 nanorods grow longer and form nanowhiskers with average aspect ratio of ~26, as shown in Figure 2b. However, it is hard to increase the aspect ratio of Na_2SO_4 nanowhiskers by further increasing the mass of $NaBH_4$, because the dissolution rate of $NaBH_4$ in EG is too slow to keep up with the growth rate of Na_2SO_4 nanowhiskers. According to a previous study,[11] dilute HCl could accelerate the dissolution rate of $NaBH_4$. We also found that the dissolving period of 0.075 g $NaBH_4$ in 50 mL EG decreases from 320 to 150 s, while the pH value of EG solution changes from 7 to 3 by adding two drops of 0.1 M HCl. In the acidic environment, the Na_2SO_4 monomer, which is consumed by the growth of Na_2SO_4 and provided by the dissolution of $NaBH_4$, is in balance, so the Na_2SO_4 nanowires with average aspect ratio beyond 100 could be obtained (Figure 2c). The above discussion suggests that the Na_2SO_4 monomer, not the H^+ concentration, holds the key for synthesizing Na_2SO_4 nanowires with high aspect ratios. A higher chemical potential generated by a higher monomer concentration is preferable for the growth of nanowires. This can be further confirmed by another experiment: with the addition of two drops of 0.1 M NaCl solution, Na_2SO_4 nanowires with aspect ratios beyond 100 could also be obtained by the reaction of 0.25 g $CuSO_4 \cdot 5H_2O$ and 0.15 g $NaBH_4$, as shown in Figure 3a. However, an extremely high

(9) (a) Dasgupta, M.; Mahanti, M. K. *Transit. Meta. Chem.* **1986**, *11*, 286–288. (b) Chen, Y. *Catal. Today* **1998**, *44*, 3–16.

(10) (a) Li, X. L.; Liu, J. F.; Li, Y. D. *Appl. Phys. Lett.* **2002**, *81*, 4832–4834. (b) Zhang, Y. W.; Yan, Z. G.; You, L. P.; Si, R.; Yan, C. H. *Eur. J. Inorg. Chem.* **2003**, *10*, 4099–4104. (c) Yu, Y.; Jin, C. H.; Wang, R. H.; Chen, Q.; Peng, L. M. *J. Phys. Chem. B* **2005**, *109*, 18772–18776.

(11) Zhang, J.; Fisher, T. S.; Gore, J. P.; Hazra, D.; Ramachandran, V. P. *Int. J. Hydrogen Energy* **2006**, *31*, 2292–2298.

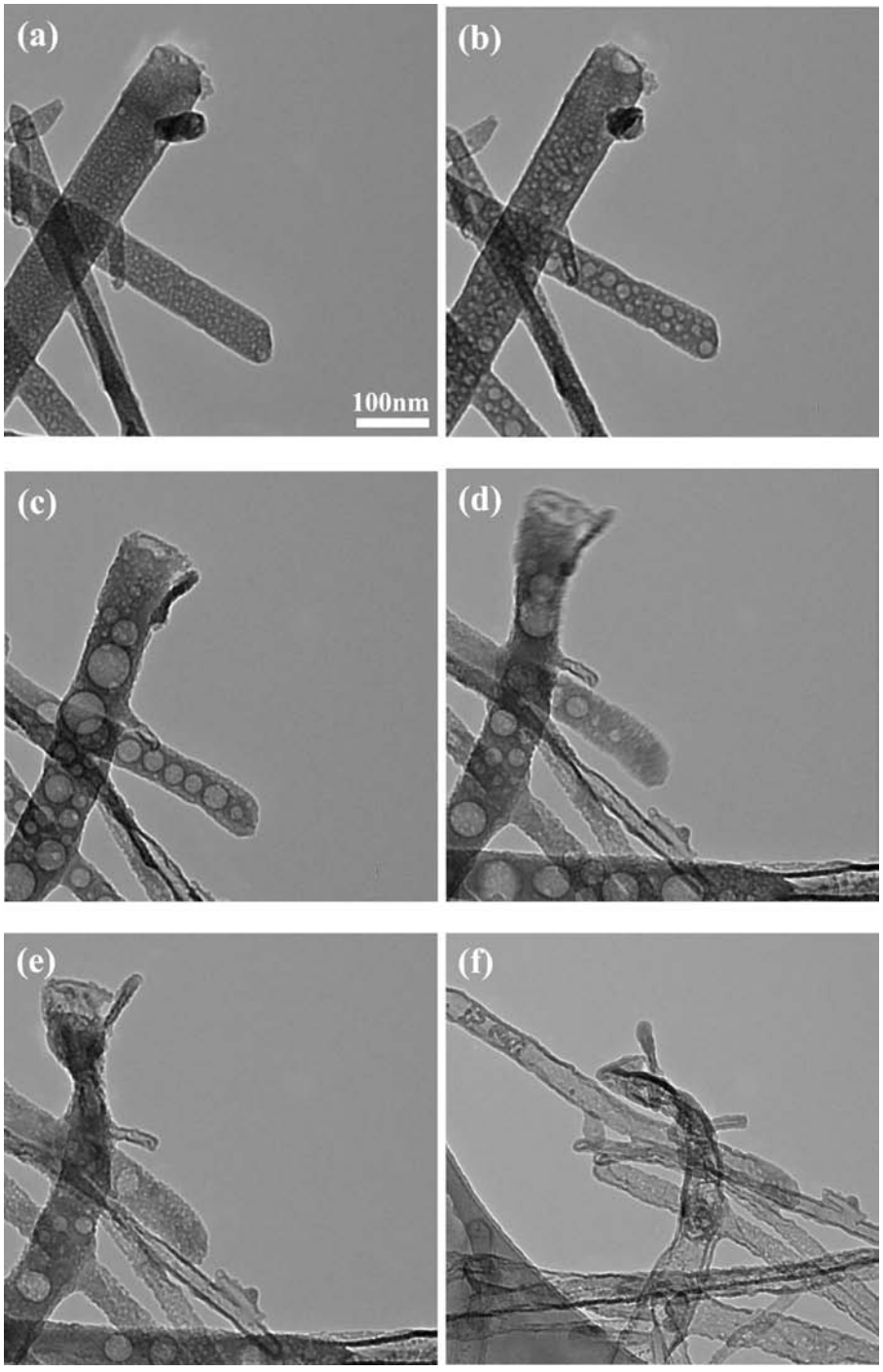

Figure 5. The structure evolutions of Na_2SO_4 nanowires by the electron beam irradiation of: (a) 30 s, (b) 2 min, (c) 6 min, (d) 8 min, (e) 10 min, and (f) 15 min.

chemical potential is disadvantageous to synthesize Na_2SO_4 nanowires. If 0.01 M H_2SO_4 reacts with 0.02 M NaOH, a high density of Na_2SO_4 nanorods with aspect ratios less than 10 is obtained, as indicated in Figure 3b. Since the neutralization reaction between H_2SO_4 and NaOH is very quick, the concentration of Na_2SO_4 monomers is highly supersaturated. A large amount of seeds form immediately, and a high nucleation rate suppresses the growth of Na_2SO_4 nanowires. According to above analysis, an optimal chemical potential is the key factor for synthesizing Na_2SO_4 nanowires with high aspect ratios. Besides the pH value and the monomer concentrations, the surfactant (PVP) also influences the growth of Na_2SO_4 nanowires. The principal role played by PVP is to suppress nucleation, thereby increasing the competitive nature of the growth. Indeed, only Na_2SO_4 nanorods can be synthesized without the help of surfactant (Figure 3c).

Figure 4 displays Na_2SO_4 submicrorods prepared by the reaction of 0.5 g $CuSO_4 \cdot 5H_2O$ with 0.3 g $NaBH_4$ and 4 mmol PVP in EG. Figure 4a clearly indicates that nanowhiskers grow coarser rather than longer with higher monomer concentration. Many Na_2SO_4 submicrorods with a diameter larger than 200 nm are synthesized. Figure 4b reveals that the obtained submicrorods have a core−shell structure; the thickness of each layer of the shell is about 10 nm. The core

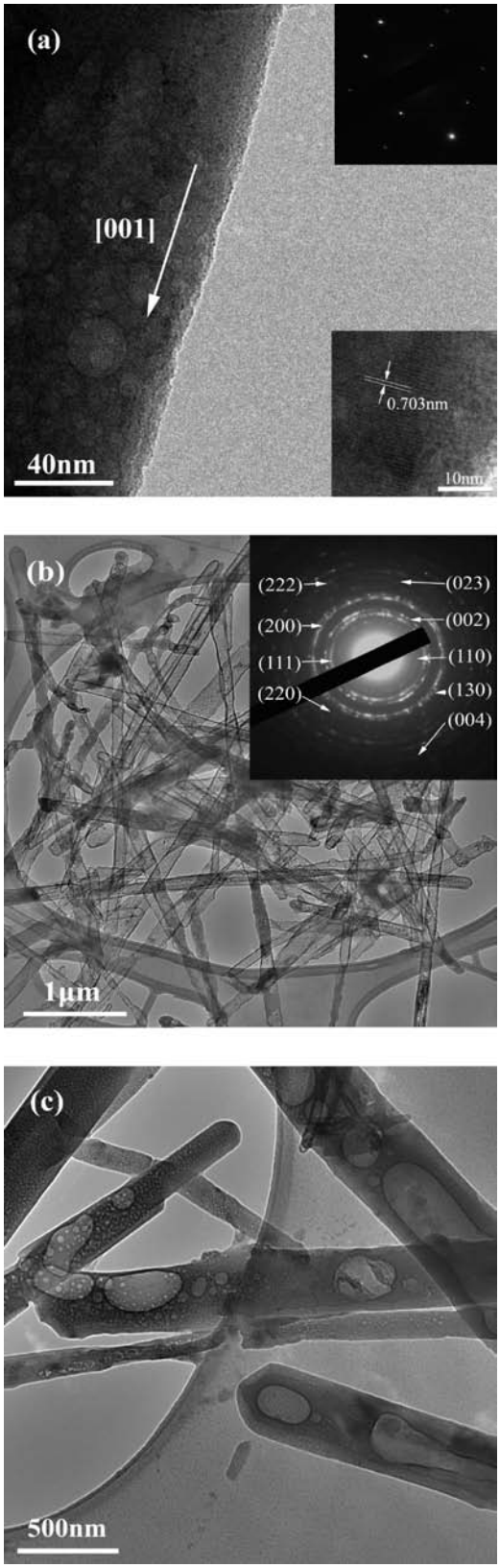

Figure 6. TEM images of Na_2SO_4 nanowires under EB irradiation. (a) A typical Na_2SO_4 nanowire after 2 min EB irradiation (200KV, 10pA). The insets are SAED pattern and the HRTEM image of this nanowire separately. (b) The irradiated Na_2SO_4 nanotubes. The inset is the SAED pattern of these nanotubes. (c) Annealed Na_2SO_4 nanowires after 60 min irradiation (200KV, 130pA).

and shell have the same crystal structure, which is confirmed by the inset diffraction pattern. The shell is crystalline Na_2SO_4 coated with amorphous materials (see Supporting Information, Figure S1). At the ends of nanowire, it is observed that the inner Na_2SO_4 nanowires are wrapped by outer Na_2SO_4 layers with identical crystal orientation. In the area indicated by arrows in Figure 4b and c, some growth edges can be clearly found. And there are notable characters of the growth edges (indicated by arrows.) of Na_2SO_4 whose outer layer can be found in Figure 4c. Figure 4d shows the transmission image of a broken Na_2SO_4 nanowire. Na_2SO_4 near the cross-section is radiolysised and left two big and several small cavities behind. There is no evidence of any liquid existing in the core of nanowire, because the liquid will vaporize immediately at the vacuum of 10^{-8} Torr in TEM.

These multilayer shell structures of Na_2SO_4 submicrorods are different from nanotubes that grow up under a "rolling mechanism".[12] We did not find this shell structure in the Na_2SO_4 nanowires, whose diameters are less than 50 nm. We conjectured that the rolling growth of Na_2SO_4 submicrorods starts from those nanowhiskers with small diameters. At the beginning of the reaction, the concentration of Na_2SO_4 monomers is higher; a higher chemical potential makes Na_2SO_4 nanorods grow into Na_2SO_4 nanowhiskers, as indicated by Figure 2b. However, due to the quick growth of Na_2SO_4 nanowhiskers, the concentration of Na_2SO_4 monomers in solution decreases quickly. Lower chemical potentials cannot provide enough driving force for the growth of Na_2SO_4 nanowhiskers, so they stop growing. With the prolonging of reaction time, more and more $NaBH_4$ is alcoholyzed. The concentration of Na_2SO_4 monomers increases again, but nanowhiskers cannot grow along their growth axes anymore because these growth surfaces are shielded by the surfactant. Comparing with the nucleation of new particles, Na_2SO_4 tends to deposit and epitaxially grow around the surface of existing Na_2SO_4 nanowires (Figure 4b and c). Such a growth process will quickly decrease the chemical potential and can also minimize the total surface energy. Finally, Na_2SO_4 submicrorods are formed, as shown in Figure 4a.

Na_2SO_4 nanowires are unstable under electron beam radiation. A series of interesting structure evolutions can be observed in a continuous electron beam irradiation of Na_2SO_4 nanowires in TEM. Figure 5 shows the structure change of Na_2SO_4 nanowires. A 200 kV electron beam with a beam intensity of 10 pA/cm^2 is targeted on a sample surface for different times. Initially the electron irradiation (for about 30 s) develops lots of small bubbles in each individual nanowire (Figure 5a). These bubbles expand, merge, and grow up under a continuous uniform irradiation from 2 to 6 min. In this course, a molten material flows in the 'core' of nanowires (Figure 5b and c). After 8 min of irradiation, some regions of the outer 'shell' were broken by the inner pressure, and the gas and molten phases in the nanowires began to vaporize (Figure 5d and e). Finally, nanotubes form after 15 min of irradiation (Figure 5f).

It is well-known that radiolysis phenomena exists in inorganic compounds under electron beam irradiation by electronic excitation.[13] Usually radiolysis happens homogeneously, however. The observed selective radiolysis is beyond

(12) (a) Li, Y. D.; Wang, J. W.; Deng, Z. X.; WU, Y. Y.; Yang, P. D. *J. Am. Chem. Soc.* **2001**, *123*, 9904–9905. (b) Sun, X. M.; Chen, X.; Li, Y. D. *Inorg. Chem.* **2002**, *41*, 4996–4498. (c) Li, Y. D.; Li, X. L.; He, R. R.; Zhu, J.; Deng, Z. X. *J. Am. Chem. Soc.* **2002**, *124*, 1411–1416.

our expectation. According to the patterns of XRD and SAED, there is no other phase in these irradiated nanowires. So we deduce that the formation of Na_2SO_4 nanotubes has a close relation with their original nanowire structures. When the Na_2SO_4 nanorods/nanowires quickly grow along the axial direction, some H^+ or other ion-related defects or impurities may be kept in inner part of the nanowires. The presence of defects and impurities makes Na_2SO_4 nanorods or nanowires sensitive to the electron beam because those defects and impurities provide preferred sites for localized excitations and locally decreased lattice binding energies [13a].

Figure 6 is some further observations of Na_2SO_4 nanowires under electron beam irradiation. When the samples are irradiated by electron beam, small bubbles first appear in the inner part of Na_2SO_4 nanowires (the gas in the bubbles may be O_2, SO_2, or H_2O) because of the higher defects and the impurities density in this region. At the same time, electron beams will result in local heating. Degradation of surfactants attached on the surfaces of nanowires will take out part of the energy and the cool from the surface of nanowires. So the inner part of Na_2SO_4 nanowires will be melted first by the EB heating and form a solid Na_2SO_4 'shell' with molten Na_2SO_4 'core'. Figure 6a shows TEM images of a typical Na_2SO_4 nanowire with [001] growth direction (the insets are the SAED pattern and the HRTEM image of this nanowire). After 2 min of EB irradiation (200KV, 10pA), bubbles are formed in the nanotubes, but the surface of nanotubes still keep the prefect crystal structure. We can observe the lattice fringes from the inset HRTEM image of the nanotube surface. The interplanar spacing is about 0.703 nm, which corresponds to the (001) plane of orthorhombic Na_2SO_4. After the expansion of the bubbles, when the pressure of gas and molten Na_2SO_4 exceed the strength limit of Na_2SO_4 'shell', the 'shell' will be broken, the inner gas and molten phase leak and volatilize immediately at the vacuum of 10^{-8} Torr, forming hollow nanotubes. These tubes are still Na_2SO_4, as confirmed by SAED pattern in Figure 6b. In order to verify our assumption, we put the same sample on a hot plate and annealed at 300 °C for 3 h. When the annealed samples were observed in the TEM again, their irradiation resistance is improved. Under a beam density of 130 pA/cm^2, the cavities appear after 3 min of irradiation. They gradually grow up and become stable after 20 min of observation. A few structure changes can be observed for another 40 min of irradiation, as indicated in Figure 6c. Neither flowing phenomena nor nanotube formation can be observed in the course. The electron dose in a unit area is proportional to the irradiation time multiplying beam density. So the irradiation resistance of Na_2SO_4 nanowires is increased more than 100 times after the annealing treatment. This result indicates that the defect density is obviously reduced by annealing.

Finally we would like to mention that the simple synthesis technology and diversity of morphology of Na_2SO_4 nanomaterials will bring some opportunities for chemistry, materials, and biology. These Na_2SO_4 nanorods, nanowhiskers, nanowires, submicrorods, and nanotubes are candidate templates for nanotubes, nanocapsule, and microcapsules by coating them with designed materials or their precursors and by removing the Na_2SO_4 with water. In addition, the simple, facile, and cheap synthetic approach developed in this paper can be extended to the preparation of other salt crystalline nanomaterials with highly anisotropic structures. And these size-controllable, environmentally friendly salt nanomaterials enrich the family of nanomaterials.

4. Conclusions

We have demonstrated the synthesis of Na_2SO_4 crystalline nanowires in bulk quantities by a simple and clean solution-based wet chemistry method. The size and aspect ratios of as-synthesized Na_2SO_4 nanowires are finely tuned by the adjustment of pH and monomer concentrations. Mechanisms for the growth processes are proposed that can explain the observations consistently. It is expected that the synthetic method employed in this work can be extended to the preparation of other crystalline one-dimensional nanomaterials with highly anisotropic structures. Our experiments also demonstrated that Na_2SO_4 nanotubes can be obtained by the selective radiolysis of Na_2SO_4 nanowires. This approach also could be used in preparing other hollow micronanostructures. Further research in preparing hollow structures with different particle size for biomedical applications is in progress.

Acknowledgment. This work is supported by the National Science Foundation Nanotechnology and Interdisciplinary Research Team (NSF NIRT) (CBET-0506830) and the NSF grant (CBET-0830098). R.T.Z. also gratefully acknowledges partial financial support from the China Scholarship Council, Beijing Nova project (2006A32) and the National Basic Research Program of China (No: 2010CB832905). We wish to thank Dr. Scott Speakman and Dr. Y. Zhang for their helpful discussion during this work.

Supporting Information Available: All the synthesis conditions and the products are listed. This material is available free of charge via the Internet at http://pubs.acs.org.

(13) (a) Hobbs, L. W.Introduction to Analytical Electron Microscopy. In *Radiation effects in analysis by TEM*; Hren, J. J., Goldstein, J. I., Joy, D. C., Eds.; Plenum: New York, 1987; pp 399−445. (b) Hobbs, L. W. *Scanning Microsc., Suppl.* **1990**, *4*, 171–183. (c) Egerton, R. F.; Crozier, P. A.; Rice, P. *Ultramicroscopy* **1987**, *23*, 305–312. (d) Egerton, R. F.; Li, P.; Malac, M. *Micron* **2004**, *35*, 399–409.